ADVANCED ENERGY MATERIALS
www.advenergymat.de

Hybrid Mg^{2+}/Li^{+} Battery with Long Cycle Life and High Rate Capability

*Tao Gao, Fudong Han, Yujie Zhu, Liumin Suo, Chao Luo, Kang Xu, and Chunsheng Wang**

Electrochemical energy storage is the core technology for the success of green transportation and renewable energy. Among existing energy-storage chemistries, magnesium-ion batteries (MIBs) are receiving growing attention in recent years since the pioneering work of Aurbach et al.,[1] due to the potential benefit of its two-electron nature and intrinsic low cost compared with lithium-ion batteries (LIBs). Additionally, magnesium (Mg) is safe to handle in ambient atmosphere,[2] and its highly reversible and dendrite-free deposition/dissolution in a Grignard-based complex electrolyte enables metallic Mg as a safe and high-capacity anode.[1,3,4] The utilization of such a metallic anode in reduction-resistant electrolytes based on ethereal solvents could not only circumvent the usage of inactive components (such as conductive material, binder, and current collectors) in a composite electrode but also eliminate the first-cycle irreversible processes associated with the solid electrolyte interface (SEI) formation in LIBs.[1] These advantages have made MIB a promising candidate system to store electrochemical energy. However, the strong Coulombic interaction between an intercalation host and the bivalent Mg^{2+} makes the solid-state diffusion of the latter rather sluggish, thus inevitably rendering MIB cathode materials as poor ion conductors.[5] This property could lead to low Mg^{2+} intercalation level, large polarization during charge/discharge, and/or rapid capacity decay for common cathode materials.[6–12] The only exception was perhaps Chevrel phases (Mo_6X_8, X = S, Se), which show acceptable intercalation kinetics and cycling stability for practical applications,[2,5] but its low voltage (1.1 V vs Mg/Mg^{2+}), low specific capacity ($C_{theoretical}$ = 128 mAh g^{-1}), and consequently low specific energy (140.8 Wh kg^{-1}) severely restrict the full potential of Mg anodes. The absence of a Mg^{2+} intercalation cathode with high voltage, high capacity, and fast kinetics has severely hindered the development of this field, making it imperative to break through this bottleneck.

One potential approach is to circumvent the intercalation of clumsy Mg^{2+} by coupling the Mg metal anode with a mature LIB cathode in a mixed Mg^{2+}/Li^{+} electrolyte. A hybrid battery chemistry thus constructed simultaneously combines the high-capacity/high-voltage LIB cathodes, fast Li^{+} intercalation, and the high-capacity/dendrite-free Mg anode (**Figure 1**a). This concept of employing multiple ions in the same electrochemical device can actually be traced back to the so-called Daniel cell, demonstrated by the British chemist John. F. Daniel in 1836. One of its successful embodiments was the recent development of highly reversible dual-graphite cells enabled by Li^{+} insertion/extraction at the anode and anions (e.g., $TFSI^{-}$) insertion/extraction at the cathode.[13,14] For aqueous batteries and supercapacitors, this concept was also proved as an effective approach to promote their performances.[15,16] Specific for MIB, Cheng et al.[17] blended lithium salt into a typical Mg complex electrolyte and observed improved rate capability in the Chevrel phase/blended electrolyte/Mg cell, in which the cathode reaction became lithiation/delithiation rather than magnesiation/demagnesiation; nevertheless, the work still did not resolve the intrinsic limitations of the Chevrel phase. A logical extension from the above concept would be to couple a conventional high-voltage/high-capacity LIB cathode with a Mg anode in a mixed-ion electrolyte. The combination would open the possibility of doubling the voltage or capacity of state-of-the-art MIB; however, it must be realized that simple replacement of the Chevrel phase with a conventional LIB cathode does not necessarily guarantee a reversible electrochemical couple with superior performance, as exemplified by the unsuccessful coupling of $LiFePO_4$ with a Mg anode in which, as shown by Yagi et al.,[18] the decomposition of electrolyte led to inferior Coulombic efficiency and rapid capacity fade.

Several aspects must be carefully examined before designing a hybrid Mg^{2+}/Li^{+} battery with high performance. First of all, the presence of lithium salt in the Mg complex electrolyte directly affects its electrochemical properties.[19–25] Despite that an anodic stability limit of 3.0 V (vs Mg/Mg^{2+}) has been reported for the Mg electrolyte all-phenyl-complex (APC),[19] this limit decreases to 2.5 V (vs Mg/Mg^{2+}) when $LiBF_4$ is added.[18] In addition, the current collector must be carefully chosen, as the corrosion of current collectors by electrolyte components could have a significant influence on the stability window of the complex electrolyte. For instance, the anodic stability of APC could be lowered to ≤2.0 V (vs Mg/Mg^{2+}), when noninert metals are used as the current collector.[26,27] Most importantly, the chosen cathode must be compatible with the complex electrolyte, i.e., it should have redox potential within the electrochemical stability window of the complex electrolyte and also remains chemically inert to electrolyte components to avoid any parasitic reactions.

With these considerations, we propose a novel hybridized Mg^{2+}/Li^{+} battery with APC-LiCl as the electrolyte, stainless steel

T. Gao, F. Han, Dr. Y. Zhu, Dr. L. Suo, C. Luo, Prof. C. Wang
Department of Chemical and Biomolecular Engineering
University of Maryland
College Park, Maryland 20740, USA
E-mail: cswang@umd.edu
Dr. K. Xu
Electrochemistry Branch, Power and Energy Division Sensor and Electron Devices Directorate
U.S. Army Research Laboratory
Adelphi, Maryland 20783, USA

DOI: 10.1002/aenm.201401507

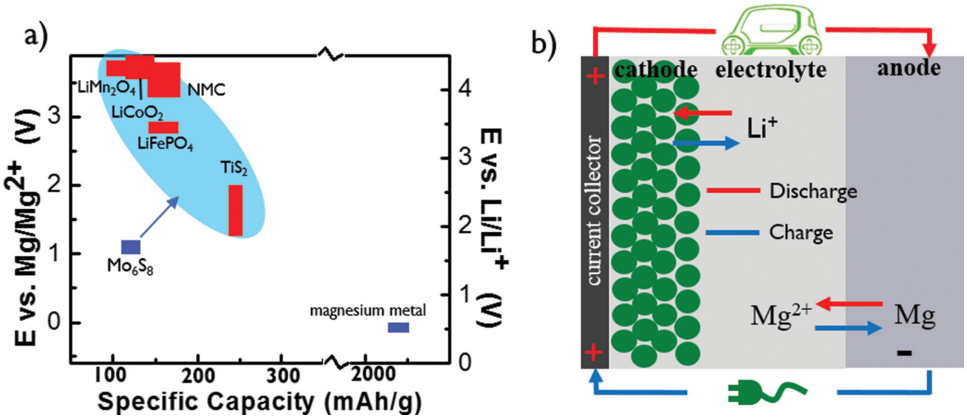

Figure 1. Schematic of a) the potential and capacity of a magnesium-ion battery's cathode (Mo_6S_8), anode (magnesium metal), and some lithium-ion battery cathodes that could possibly be used in the mixed-ion battery; b) the operating mechanism of the mixed-ion battery.

as the current collector, TiS_2 as the cathode, and Mg foil as the anode. Since the lithium-salt anion, Cl^-, is a part of APC's composition, LiCl was expected to exhibit good compatibility with APC. It has been demonstrated that APC-LiCl can support highly reversible Mg deposition/dissolution as well as provide high anodic stability despite the reaction between Lewis base LiCl and the complex Mg electrolyte.[16,20] For practical applications, stainless steel was chosen as the current collector that lowers the anodic stability of the electrolyte to 2.0 V (vs Mg/Mg^{2+}) but eliminates the utilization of expensive noble metals. LIB cathodes with lithiation/delithiation potential below 2.0 V (vs Mg/Mg^{2+}) were screened, and layered TiS_2 was identified as a model cathode due to its relatively high voltage (1.0–1.6 V vs Mg/Mg^{2+}), large capacity (240 mAh g^{-1}), high reversibility, and good compatibility with the Mg^{2+}/Li^+ complex electrolyte.

The APC-LiCl complex was revealed to be able to dissociate Li^+ and Mg^{2+}.[16] The proposed working mechanism is shown in Figure 1b. During discharge, Li^+ is inserted into TiS_2 (Equation (1)) and Mg is dissolved from Mg foil into electrolyte (Equation (2)), while during charge Li^+ is extracted from lithiated TiS_2 (Equation (1)) and Mg is deposited onto Mg foil (Equation (2)). The full cell reaction is given in Equation (3).

$$\text{Cathode}: \quad TiS_2 + Li^+ + e^- \leftrightarrow LiTiS_2 \tag{1}$$

$$\text{Anode}: \quad 0.5\,Mg \leftrightarrow 0.5\,Mg^{2+} + e^- \tag{2}$$

$$\text{Fullcell}: \quad TiS_2 + Li^+ + 0.5\,Mg \leftrightarrow LiTiS_2 + 0.5\,Mg^{2+} \tag{3}$$

To confirm that only Li^+ rather than Mg^{2+} intercalates into TiS_2 in the mixed-ion electrolyte, control experiments were conducted in three different cells with TiS_2 as the cathode: (1) a $TiS_2|Li^+|Li$ LIB using LiCl-THF electrolyte and Li anode; (2) a $TiS_2|Mg^{2+}|Mg$ MIB using APC electrolyte and Mg anode; and (3) a $TiS_2|Li^+, Mg^{2+}|Mg$ hybrid battery using APC-LiCl electrolyte and Mg anode. **Figure 2**a shows the galvanostatic charge/discharge curves of TiS_2 cathodes in these three different cells. In the $TiS_2|Li^+|Li$ cell, the lithiation/delithiation curve of TiS_2 in LiCl-THF electrolyte is almost identical to that of TiS_2 in $LiPF_6$-EC-DEC electrolyte (Supporting Information Figure S1), demonstrating that Li^+ can reversibly intercalate/deintercalate into TiS_2 in LiCl-THF electrolyte in the same manner as in a typical LIB electrolyte. On the contrary, TiS_2 barely delivers any capacity in the $TiS_2|Mg^{2+}|Mg$ cell, showing that Mg^{2+} could not intercalate into TiS_2 structure, which is consistent with the results obtained by Amir et al.[12] Nevertheless, in the $TiS_2|Li^+, Mg^{2+}|Mg$ cell, similar charge/discharge curves and a comparable capacity as that in the $TiS_2|Li^+|Li$ cell were shown, indicating similar solid solution reaction in the hybrid cell. The charge/discharge curve of the hybrid $TiS_2|Li^+, Mg^{2+}|Mg$ cell at different cycles is given in Figure 2b. Despite a low Coulombic efficiency (90%) is observed in the first cycle, the hybrid battery shows highly reversible performance in the subsequent cycles. This low initial Coulombic efficiency of TiS_2 was also noticed in the early work of Whittingham,[28] as well as in our control experiment (Supporting Information, Figure S1). Since the complex electrolyte APC-LiCl is stable within the operating window of TiS_2,[16] the low initial Coulombic efficiency is attributed to the partial trapping of the inserted lithium ions during the 1st charge. To address the problem, prelithiated TiS_2 or cathode materials with high initial cycle Coulombic efficiency could be used. The "Li^+ only intercalation" mechanism at cathode was further verified by comparing powder X-ray diffraction (XRD) patterns of TiS_2 electrode before and after discharging (Figure 2c). The wide broadening peaks at $2\theta = 13°$ and 20° arose from the air-tight sample holder. The XRD pattern of the pristine sample is in good agreement with JCPDS-15–0853, indicating the high crystallinity of TiS_2. After discharge, the pattern can be well indexed to $LiTiS_2$ (JCPDS-28–0595), confirming that only Li^+ could be inserted into TiS_2 in the mixed-ion electrolyte.

The electrochemical performance of the APC-LiCl complex electrolyte was examined by cyclic voltammetry (CV) (Figure 2d), and the morphology and composition of the deposition from the electrolyte were investigated by scanning electron microscopy (SEM) (Figure 2e) and XRD (Figure 2f). CV was conducted in a three-electrode cell with Pt foil as working electrode and two Mg foils as reference and counter electrodes. Mg^{2+} started to deposit on Pt during the cathodic scan to –0.2 V (vs Mg/Mg^{2+}) and the deposition product started to dissolve, when voltage exceeded –0.1 V (vs Mg/Mg^{2+}) during the reverse

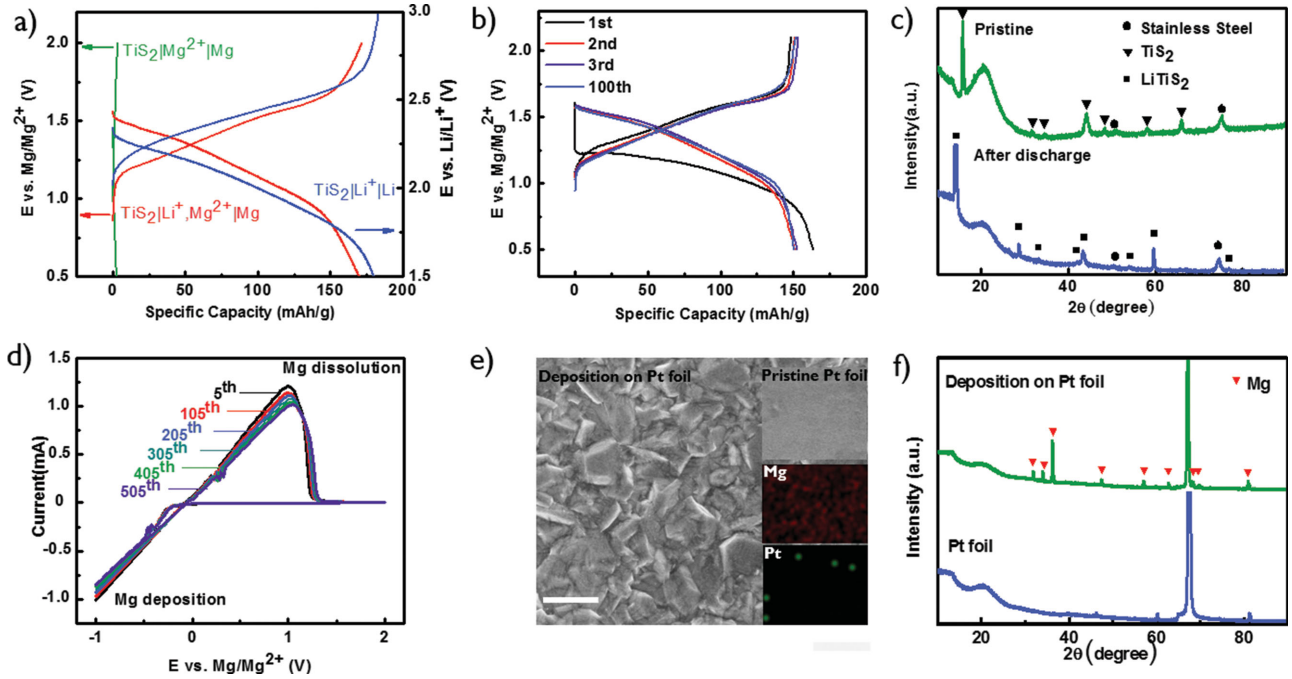

Figure 2. a) Discharge/charge curves of TiS_2 cathode in the $TiS_2|Mg^{2+}|Mg$ cell (1st cycle), $TiS_2|Li^+|Li$ cell (1st cycle), $TiS_2|Li^+$, $Mg^{2+}|Mg$ cell (2nd cycle) at 0.1 C (C = 240 mAh g^{-1}); b) discharge/charge curves of TiS_2 cathode in the $TiS_2|Li^+$, $Mg^{2+}|Mg$ cell at C/3 at different cycles; c) X-ray diffraction patterns of pristine TiS_2 electrode and TiS_2 electrode after discharge in a $TiS_2|Li^+$, $Mg^{2+}|Mg$ cell; d) cyclic voltammetry of the mixed Mg^{2+}/Li^+ electrolyte in a three-electrodes system, WE: Pt foil; RE and CE: Mg foil, scan rate: 100 mV s^{-1}; e) scanning electron microscopy (SEM) image and f) X-ray diffraction patterns of pristine Pt foil and the deposition on Pt foil after 3 h constant voltage at –0.5 V vs Mg/Mg^{2+} in the mixed Mg^{2+}/Li^+ electrolyte. Scale bar: 10 μm. Inset in e): Pristine Pt foil and Energy-dispersive X-ray spectroscopy (EDS) mapping for Mg and Pt elements of the deposition. The capacity is calculated based on the mass of TiS_2.

scan. The deposition/dissolution of Mg was highly reversible for hundreds of cycles. The effect of LiCl on the electrochemical behavior of the complex electrolyte has been thoroughly studied by Gofer et al.,[20] who pointed out that the presence of LiCl did not alter the shape of the curve or the charge balance of deposition/dissolution, but slightly affected the overpotential for deposition. To examine the chemical composition of the deposit from the Mg^{2+}/Li^+ mixed-ion electrolyte, XRD patterns of the Pt working electrode were recorded before and after electrochemical depositing in the APC-LiCl electrolyte (Figure 2f). After 3 h of deposition, all XRD peaks of the deposition can be assigned to Mg except for the peaks of the sample holder and Pt substrate. No peaks can be indexed to Li or Mg–Li alloy. Electron energy loss spectroscopy (EELS) result further verifies that no Li can be detected in the deposition (Supporting Information Figure S2). Although Li^+ might electrochemically react with the deposited Mg to form Li–Mg alloy in the potential range of Mg depositing,[29] the results of this work confirm that the deposition was pure magnesium with no detectable lithium, in excellent agreement with Gofer's work.[20] The surface morphology of the deposit from the APC-LiCl complex electrolyte was also examined under SEM, which reveals that no dendrite but micron-sized uniform scale-like deposition was formed (Figure 2e). This particular dendrite-free deposition from the Grignard-reagent-based or other organometallic complex electrolytes has been well reported by Aurbach et al.[3] and Matsui et al.[4] both experimentally and theoretically, and a mechanism was proposed based on the crystallographic nature of Mg metal: Mg prefers high-dimensional uniform deposition, while Li prefers one dimensional dendrite formation.[19,30–33]

The cycling stability and rate capability of the hybrid Mg battery are shown in **Figure 3**. Due to the simultaneous reversibilities of Mg deposition/dissolution at Mg anode and Li^+ intercalation/deintercalation at TiS_2 cathode, as well as the chemical inertness of TiS_2 toward the complex electrolyte, no capacity decay can be observed for at least 400 cycles with Coulombic efficiency as high as 99.5% except for the first few cycles, demonstrating the best cycling stability among reported MIBs and mixed Mg^{2+}/Li^+ batteries using non-Mo_6X_8 cathodes.[2,5,18] Compared to the MIB using $Mo_6\times_8$ cathode, the theoretical specific capacity and specific energy of the mixed-ion battery are 161.0 mAh g^{-1} and 209.3 Wh kg^{-1} even when the weight of lithium salt was taken into account, which are 32.2% and 56.2% higher than 121.8 mAh g^{-1} and 134 Wh kg^{-1} of the state-of-the-art MIB (see Supporting Information for detailed calculation). A comparison on specific capacity/specific energy between LIB, MIB, and the hybrid battery is given in the Supporting Information, Figure S3. Electrochemical impedance spectroscopy tests were conducted to analyze the kinetics of the hybrid battery (Supporting Information, Figures S4 and S5). Although the hybrid battery inherits the fast kinetics of lithium intercalation/deintercalation at cathode, it exhibits lower rate capability than LIB due to relatively slow Mg dissolution/deposition. Utilizing nanosized Mg metal was demonstrated to be a useful method to address this limitation owing to the dramatically increased reaction area.[7] Nevertheless, an enhanced rate capacity is still

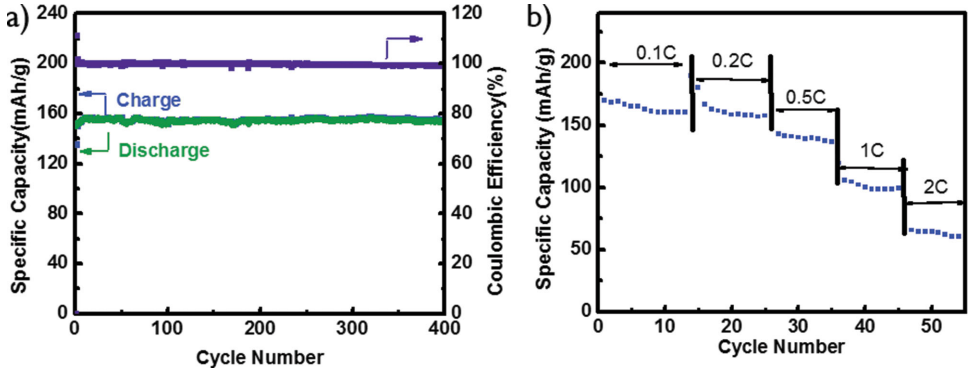

Figure 3. a) Cycling stability at C/3 and b) rate capability of a TiS_2|Li^+, Mg^{2+}|Mg battery.

observed compared with MIB, as demonstrated in Figure 3b.[34] Hence, the proposed hybrid Mg battery shows an overall superior performance than the traditional MIB.

In conclusion, a highly reversible hybrid battery with a Mg anode and LIB cathode through rational design is reported. In terms of specific capacity, specific energy, cycling stability, and rate capability, the reported hybrid Mg^{2+}/Li^+ battery demonstrates the best overall performance among reported magnesium-based batteries.[2,5,26,27,34] The intrinsic challenges of dendrite growth in lithium batteries and poor Mg^{2+} insertion/extraction kinetics in MIBs have been simultaneously circumvented in this hybrid chemistry. Noteworthily, there is still a huge potential to be exploited for this hybrid battery concept, since recent discoveries of enhanced electrolyte stability on commercially feasible current collectors have made the application of cathodes with higher voltage possible.[27] If a compatible high-voltage electrolyte–cathode pair can be found, the specific energy of the hybrid battery could be potentially doubled (385.2 Wh kg^{-1}). This makes the hybrid battery an alternative that could be even competitive against the mainstream LIB technology (400 Wh kg^{-1}) (see Supporting Information), not mentioning the advantages of a dendrite-free Mg anode that is free of inert masses (current collector, binder, and conductive additives) and first-cycle irreversible reactions associated with SEI formation. Since all Li^+ ions are provided by the electrolyte, a high Li^+ concentration is required for the hybrid battery to function at high capacities. A systematic evaluation of the lithium salt concentration effect on the hybrid battery's performance is underway.

Experimental Section

Electrolyte Synthesis: The synthesis of electrolytes was conducted under pure argon atmosphere in VAC, Inc. glove box (<1 ppm of water and oxygen). The solvent, anhydrous THF (Aldrich, 99.9%, inhibitor free), was dried with molecular sieve (5 Å, Aldrich) in glove box overnight before filtering. The electrolyte in control experiment (1), 0.4 M LiCl in THF, was prepared by dissolving LiCl (Aldrich, 99%) into THF. The electrolyte in control experiment (2), 0.4 M APC, was prepared by first dissolving $AlCl_3$ (Aldrich, 99.999%) into THF followed by adding the solution dropwisely into PhMgCl solution (Aldrich, 2.0 M in THF) and stirring overnight. The electrolyte in control experiment (3), 0.4 M APC-LiCl, was prepared by dissolving LiCl into the synthesized APC electrolyte.

Electrochemical Measurement: Galvanostatic tests were carried out in 2025 coin cells with Land CT 2001A. Micron-sized TiS_2 powder (Aldrich, 99.9%, 200 mesh) were mixed with carbon black (Super P) and sodium alginate (MP, Biomedicals) in an 80:10:10 wt% ratio, hand-milled for 30 min, and then casted onto individual stainless steel disk (TBI, 0.001 in. thickness). The loading for each electrode is ~1.0 mg. The electrode disks were dried in a vacuum oven at 100 °C overnight. Li foil and Mg ribbon were used as anodes in LIB and MIB/mixed-ion battery. Celgard 3501 was used as the separator. CV was performed on Gamry Reference 3000 with a scan rate of 100 mV s^{-1}, and –1 and 2 V (vs Mg/Mg^{2+}) were used as high and low cutoff voltages when testing the APC-LiCl electrolyte.

Material Characterization: The morphology of the deposition in APC-LiCl complex electrolyte was examined using a Hitachi SU-70 field-emission scanning electron microscope. X-ray powder diffraction patterns were obtained on Bruker Smart 1000 (Bruker AXS Inc., USA) by using Cu$K\alpha$ radiation with an air-tight holder from Bruker. Electron energy loss spectroscopy results were obtained on JEOL JEM 2100F TEM/STEM.

Supporting Information

Supporting Information is available from the Wiley Online Library or from the author.

Acknowledgements

This work was supported by DoE ARPA-E (DEAR0000389). The authors acknowledge the support of the Maryland NanoCenter and its NispLab. The NispLab is supported in part by the NSF as a MRSEC Shared Experimental Facility.

Received: August 27, 2014
Revised: September 26, 2014
Published online:

[1] D. Aurbach, Z. Lu, A. Schechter, Y. Gofer, H. Gizbar, R. Turgeman, Y. Cohen, M. Moshkovich, E. Levi, *Nature* **2000**, *407*, 724.
[2] H. D. Yoo, I. Shterenberg, Y. Gofer, G. Gershinsky, N. Pour, D. Aurbach, *Energy Environ. Sci.* **2013**, *6*, 2265.
[3] D. Aurbach, A. Schechter, M. Moshkovich, Y. Cohen, *J. Electrochem. Soc.* **2001**, *148*, A1004.
[4] M. Matsui, *J. Power Sources* **2011**, *196*, 7048.
[5] E. Levi, Y. Gofer, D. Aurbach, *Chem. Mater.* **2010**, *22*, 860.

[6] R. Zhang, X. Yu, K. W. Nam, C. Ling, T. S. Arthur, W. Song, A. M. Knapp, S. N. Ehrlich, X. Q. Yang, M. Matsui, *Electrochem. Commun.* **2012**, *23*, 110.
[7] Y. Liang, R. Feng, S. Yang, H. Ma, J. Liang, J. Chen, *Adv. Mater.* **2011**, *23*, 640.
[8] Y. NuLi, J. Yang, Y. Li, J. Wang, *Chem. Commun.* **2010**, *46*, 3794.
[9] P. Novak, J. Desilvestro, *J. Electrochem. Soc.* **1993**, *140*, 140.
[10] Y. Nuli, Z. P. Guo, H. K. Liu, J. Yang, *Electrochem. Commun.* **2007**, *9*, 1913.
[11] W. Y. Li, C. S. Li, C. Y. Zhou, H. Ma, J. Chen, *Angew. Chem. Int. Ed.* **2006**, *45*, 6009.
[12] N. Amir, Y. Vestfrid, O. Chusid, Y. Gofer, D. Aurbach, *J. Power Sources* **2007**, *174*, 1234.
[13] J. A. Read, A. V. Cresce, M. H. Ervin, K. Xu, *Energy Environ. Sci.* **2014**, *7*, 617.
[14] S. Rothermel, P. Meister, G. Schmuelling, O. Fromm, H. Mayer, S. Nowak, M. Winter, T. Placke, *Energy Environ. Sci.* **2014** , *7*, 3412.
[15] J. Yan, J. Wang, H. Liu, Z. Bakenov, D. Gosselink, P. Chen, *J. Power Sources* **2012**, *216*, 222.
[16] H. D. Yoo, I. Shterenberg, Y. Gofer, R. E. Doe, C. C. Fischer, G. Ceder, D. Aurbach, *J. Electrochem. Soc.* **2014**, *161*, A410.
[17] Y. Cheng, Y. Shao, J. Zhang, V. L. Sprenkle, J. Liu, G. Li, *Chem. Commun.* **2014**, *50*, 9644.
[18] S. Yagi, T. Ichitsubo, Y. Shirai, S. Yanai, T. Doi, K. Murase, E. Matsubara, *J. Mater. Chem. A.* **2014**, *2*, 1144.
[19] O. Mizrahi, N. Amir, E. Pollak, O. Chusid, V. Marks, H. Gottlieb, L. Larush, E. Zinigrad, D. Aurbach, *J. Electrochem. Soc.* **2008**, *155*, A103.
[20] Y. Gofer, O. Chusid, H. Gizbar, Y. Viestfrid, H. E. Gottlieb, V. Marks, D. Aurbach, *Electrochem. Solid-State Lett.* **2006**, *9*, A257.
[21] R. Mohtadi, M. Matsui, T. S. Arthur, S. J. Hwang, *Angew. Chem. Int. Ed.* **2012**, *51*, 9780.
[22] Y. S. Guo, F. Zhang, J. Yang, F. F. Wang, Y. NuLi, S. I. Hirano, *Energy Environ. Sci.* **2012**, *5*, 9100.
[23] R. E. Doe, R. Han, J. Hwang, A. J. Gmitter, I. Shterenberg, H. D. Yoo, N. Pour, D. Aurbach, *Chem. Commun.* **2014**, *50*, 243.
[24] T. J. Carter, R. Mohtadi, T. S. Arthur, F. Mizuno, R. G. Zhang, S. Shirai, J. W. Kampf, *Angew. Chem. Int. Ed.* **2014**, *53*, 3173.
[25] O. Chusid, Y. Gofer, H. Gizbar, Y. Vestfrid, E. Levi, D. Aurbach, I. Riech, *Adv. Mater.* **2003**, *15*, 627.
[26] S. Yagi, A. Tanaka, Y. Ichikawa, T. Ichitsubo, E. Matsubara, *J. Electrochem. Soc.* **2013**, *160*, C83.
[27] Y. Cheng, T. Liu, Y. Shao, M. H. Engelhard, J. Liu, G. Li, *J. Mater. Chem. A* **2014**, *2*, 2473.
[28] M. S. Whittingham, *Prog. Solid-State Chem.* **1978**, *12*, 41.
[29] Z. Shi, M. L. Liu, D. Naik, J. L. Gole, *J. Power Sources* **2001**, *92*, 70.
[30] D. Aurbach, Y. Cohen, M. Moshkovich, *Electrochem. Solid-State Lett.* **2001**, *4*, A113.
[31] D. Aurbach, H. Gizbar, A. Schechter, O. Chusid, H. E. Gottlieb, Y. Gofer, I. Goldberg, *J. Electrochem. Soc.* **2002**, *149*, A115.
[32] D. Aurbach, R. Turgeman, O. Chusid, Y. Gofer, *Electrochem. Commun.* **2001**, *3*, 252.
[33] C. Ling, D. Banerjee, M. Matsui, *Electrochim. Acta* **2012**, *76*, 270.
[34] D. Aurbach, G. S. Suresh, E. Levi, A. Mitelman, O. Mizrahi, O. Chusid, M. Brunelli, *Adv. Mater.* **2007**, *19*, 4260.